Journal of Applied Sciences and Nanotechnology

Journal homepage: jasn.uotechnology.edu.iq

Expired Dexon Drug as Green Inhibitor for Carbon Steel in Simulated Seawater Medium

[1]Shams A. Naji, [2]Rana Afif Anee*, [3]Sadeer M. Majeed

[1]Ministry of Environment, Iraq
[2]Department of Material Engineering, University of Technology – Iraq, Iraq
[3]Department of Applied Sciences, University of Technology – Iraq, Iraq

A R T I C L E I N F O

Article history:
Received: August, 21, 2024
Accepted: November, 16, 2024
Available online: December, 10, 2024

Keywords:
Dexon drug inhibition,
Green materials,
Sustainability,
Dexamethasone

Corresponding Author:
Rana Afif Anee
dr.rana_afif@yahoo.com

A B S T R A C T

The addition of expired drugs as green inhibitors takes high attention as an alternative material compared with other expensive, toxic, non-available chemical inhibitors. In this study, the Dexon drug was suggested as a green inhibitor for commonly used carbon steel in (3.5% NaCl solution) within a temperature range of 303 to 333 K. Corrosion/inhibition investigation was done by potentiostatic analysis to record the corrosion potential, corrosion current density, and Tafel slopes for the added four concentrations (4, 20, 40 and 60 mL/L) of the drug. The polarization resistances and inhibition efficiencies reached the highest value of (25.86×10^{-3} Ω.cm^2) and (95.57%) respectively for 60 mL/L at 303 K. For examination of inhibited surface, Infrared spectrum, electron scanning microscopy, and atomic force microscopy. These techniques confirmed effective surface coverage by the adsorbed drug, forming a (Fe^{2+} – Dexamethasone) complex. This was further supported by a reduction in surface roughness from 270.8 nm to 24.96 nm following inhibition using a concentration of 60 mL/L. Theoretical calculations indicated that the adsorption process was physical, spontaneous, less disordered, and exothermic. Additionally, quantum data, including HOMO and LUMO analyses, demonstrated the high adsorption capability of the Dexamethasone molecule on the steel surface. The results showed an energy gap of 3.43 eV, reflecting the molecule's soft nature and the release of energy during the adsorption process.

https://doi.org/10.53293/jasn.2024.7485.1314, Department of Applied Sciences, University of Technology - Iraq.

1. Introduction

Corrosion inhibition is one of four main techniques used to reduce, minimize, limit, control, or prevent the dissolution of metals and alloys. Among these techniques, material selection is the first approach for corrosion prevention. In terms of corrosion control, this typically involves avoiding the presence of galvanic elements in the main structural materials. Also, it includes other secondary materials and insulation to avoid galvanic corrosion, which is determined by material functional features such as geometry, surface conditions, production,

environmental factors, and mechanical loads in addition to the corrosion properties. The design and material selection processes are interconnected, meaning that individual components, structures, and their surroundings must be taken into consideration. The third technique is electrical protection, which includes cathodic and anodic protection. The principle of cathodic protection involves applying an external current to the material, shifting its potential into the immune region. In contrast, anodic protection aims to keep the material in the passive region, based on its polarization behavior as shown in the (Tafel plot). The application of coatings to prevent corrosion works by three main mechanisms including (i) Barrier effect which prevents any contact between the corrosive electrolyte and the metallic material; (ii) Cathodic protection through applying the coating material as a sacrificial anode; and (iii) Inhibition/passivation, similar to anodic protection, where the coating helps maintain the material in a passive state [1]. Finally, the chemical inhibitors to prevent corrosion are quite varied and can serve as the first line of defense against corrosion in certain applications. However, there is no standard rule for applying this technique; it depends on scientific studies, trial-and-error experiments in both laboratory and field conditions, along the application of established equations, rules, and theories to identify and evaluate potential inhibitor materials. Many chemical materials were tested as corrosion inhibitors including organic and inorganic, natural and synthetic, long chains and aromatic, and small molecules and bulky others. In the last decades, there has been growing attention on the use of green, natural, and sustainable materials especially plant extracts and drugs [2].

Numerous studies between 2010 and 2024 have focused on the use of drugs as corrosion inhibitors for important metals and alloys like carbon steel, aluminum, copper, zinc, and brass. Notable works include Nnabuk *et al*. using (norfloxacin, ciprofloxacin, ofloxacin and sparfloxacin) [3], Eddy and Ebenso using (Tarivid) [4], Abdel Hameed using (Ranitidine) [5], Imran et al. using (Cefixime) [6], Abd Allah *et al*. using some antihypertensive drugs [7], Fouda *et al*. using (Septaitzole) [8], Fouda *et al*. using some antibiotic derivatives [9], Fouda and Gadow using some antibiotic drugs [10], Mahdi using (Amoxicillin) [11], Akpan and Offiong using (Amodiaquine) [12], Abdel Hameed *et al*. using (Voltaren) [13], Paul and Umar using (Cefuroxime axetil) [14], Attla using (Farcolin) [15], Abdallah *et al*. using some antibiotic drugs [16], Abdelaziz *et al*. using (Augment)[17], Raheem using (Amoxicillin, Cephalexin and Cefixim) [18], Motawea *et al*. using (Cidamex) [19], Fouda *et al*. using (Meropenem) [20], Singh *et al*. using (Atorvastatin) [21], Verma and Khan using (Sulfacetamide and Sotalol) [22], Verma *et al*. using some commercially drugs [23], Ikpi *et al*. using (Levofloxacin) [24], Anaee *et al*. using (Etoricoxib) [25] and (Metoclopramide) [26], Akram *et al*. using (Cefoperazone) [27], Thekra *et al*. using (Spiramycin) [28-30], Hiba *et al*. using (Metheprim) [31], Saja *et al*. using (Ca tablet and D3) [32, 33], and Al-Ghaban *et al*. using (Butamirate) [34]. Dexon Syrup is one of many drugs used to treat cough and can be taken with or without food, with the dosage and duration determined by a doctor based on the patient's condition. This drug has some side effects including nausea, diarrhea, bloating, indigestion, sweating, headache, and skin rash. Therefore, it is not recommended to take the medication without a doctor's advice. The dosage is typically measured using a cup, and the syrup should be well-shaken before use. This means that this may expire within a short period after opening and must be disposed of. This study suggested using Dexon Syrup as a corrosion inhibitor for carbon steel in saline conditions (3.5% NaCl) at four different temperatures and four various concentrations. The investigation was done by corrosion measurement using Potentiostat supported by other techniques for surface characterization.

2. Experimental Procedure

2.1 Materials and Chemicals

Many specimens of carbon steel were used as a substrate that was cut with a dimension of ($20 \times 20 \times 4\ mm$), followed by applying some steps to these specimens including grinding with SiC paper, polishing with Al_2O_3 paste and kept them for electrochemical tests. 3.5% $NaCl$ was used as a corrosive solution which was prepared by dissolving $17.5\ gm$ of sodium chloride (From $Loba\ Chemie\ PVT.LTD.$) in $500\ mL$ of distilled water. Dexon drug from the national company (SDI Samarra) in Iraq was investigated as an inhibitor by adding four concentrations (4, 20, 40, and 60 mL/L) to a corrosive solution at four different temperatures (303, 313, 323 and 333 K) which controlled by a water bath. The chemical formula of (dexamethasone) is shown in Fig. 1.

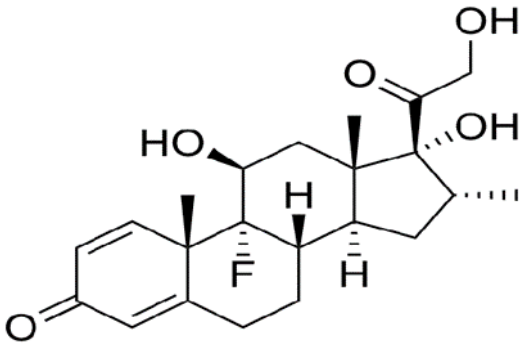

Figure 1: Chemical formula of dexamethasone.

2.2 Characterization Tests

To support the corrosion/inhibition test, many techniques can be used to characterize the inhibited surface including Fourier Transform Infrared Spectroscopy (FTIR) from Bruker company using an ATR mode to identify the composition of the drug and the film formed on a steel surface after inhibition. Scanning electron microscopy (SEM) from TESCAN company was used to identify the corroded and inhibited carbon steel surface. Atomic force microscopy (AFM) from (Nanosurf Switzerland) was utilized to investigate the topographical feature and other parameters for corroded and inhibited carbon steel surfaces.

2.3 Electrochemical Test

The electrochemical properties of carbon steel were investigated by recoding the open circuit potential (E_{oc}), the corrosion potential (E_{corr}), the corrosion current density (i_{corr}) and Tafel slopes (b_c& b_a) using a three-electrodes cell with controlled temperature by jacket cell connected to Potentiostat from (Corrtest, model CS350). The (E_{oc}) was recorded after 600 sec. immersion in (3.5% NaCl) followed by recording the polarization curve (Tafel plot) by applying $\pm$ 0.2 V at a scan rate of 1 mV/sec [35, 36]. Other corrosion parameters were calculated including the polarization resistance (R_p) as follow [37, 38]:

$$\boldsymbol{R_p = \frac{b_c \times b_a}{2.303\, i_{corr}(b_c + b_a)}} \qquad \textbf{(1)}$$

And by using current densities without inhibitors (i_{corr}) and with inhibitor (i'_{corr}), the inhibition efficiencies ($IE\%$) for inhibitors were also calculated as follows [39][40]:

$$\boldsymbol{IE\% = \left[1 - \frac{i'_{corr}}{i_{corr}}\right] \times 100} \qquad \textbf{(2)}$$

2.4 Theoretical Calculations

Some theoretical calculations can be added to support the experimental measurements involved in the adsorption isotherm properties including adsorption./desorption constant (K_{ads}) using the data of the coverage (θ) and the concentration of the used inhibitor of the drug (C_{drug}) as follows [41]:

$$\boldsymbol{\theta = \left(\frac{IE}{100}\right)} \qquad \textbf{(3)}$$

$$\boldsymbol{K_{ads} = \frac{\theta}{C_{drug}(1-\theta)}} \qquad \textbf{(4)}$$

After that, the apparent free adsorption energy (ΔG^o_{ads}) can be calculated as follows:

$$\boldsymbol{\Delta G^o_{ads} = -2.303\, RT(\log 55.5 \times K_{ads})} \qquad \textbf{(5)}$$

Followed by the prediction of other thermodynamic data for the adsorption process including the entropy (ΔS^{o}_{ads}) and enthalpy (ΔH^{o}_{ads}) as follows:

$$\Delta \mathbf{S^{o}_{ads}} = -\left[\frac{\partial(\Delta \mathbf{G^{o}_{ads}})}{\partial \mathbf{T}}\right] \quad \textbf{(6)}$$

$$\Delta \mathbf{G^{o}_{ads}} = \Delta \mathbf{H^{o}_{ads}} - \mathbf{T}\Delta \mathbf{S^{o}_{ads}} \quad \textbf{(7)}$$

Also, the electronic properties for inhibitor's molecule by quantum calculations were investigated for Dexon's molecule to show the sites related to inhibition role using (Gaussian 09, Revision D.01) with basis set (6-311G) [42-44] as well as using the Becke three-parameter hybrid (B3) [45] and the Lee-Yang-Parr (LYP) correlation functional (B3LYP) [46].

Some theoretical data were calculated by the density function theory (DFT) method using some formulas including Ionization potential (I), Electron affinity (A), Hardness (η), Softness (σ), Electronegativity (χ), Chemical potential (μ), Electrophilicity (ω) and Fraction of electrons transported (ΔN) were calculated according to the below equations [41]:

$I = -E_{HOMO}$,

$A = -E_{LUMO}$,

$\eta = \frac{I-A}{2}$,

$\sigma = \frac{1}{2\eta}$,

$\chi = \frac{I+A}{2}$,

$\mu = -\chi$,

$\omega = \frac{\chi^2}{2\eta}$,

$$\Delta \mathbf{N} = \frac{\chi_{Fe} - \chi_{Inh}}{2(\eta_{Fe} + \eta_{Inh})} \quad \textbf{(8)}$$

Where: (E_{HOMO}) is the highest occupied molecular orbital energy and (E_{LUMO}) the lowest unoccupied molecular orbital energy.

3. Results and Interpretations

3.1. Corrosion/Inhibition Results

The addition of any inhibitor aims to reduce the corrosion process by reducing the dissolution of metals from the substrate through the formation of a barrier depending on the inhibitor's nature. In the case of organic molecules, the feature of hydrocarbons supported by functional groups plays a vital role in adsorbing on this substrate, the prediction of this process can be achieved during the polarization curves in the absence (Blank) and the presence (Inhibited solution) of inhibitor as illustrated in Fig. 2. The presence of inhibitors in almost all concentrations led to shifting the curves towards the noble direction and lower current values, i.e., minimizing the dissolution of iron atoms (Fe) to iron ions (Fe^{2+}) and in contrast, minimizing the conversion of oxygen molecules (O_2) to hydroxyl ions (OH^-) at anodic and cathodic sites respectively. This process leads to the form of some complexes between iron ions (Fe^{2+}) and drug molecules ($C_{22}H_{29}FO_5$), in the presence of five oxygen atoms and one flour atom, the Dexon molecules can orient toward Fe(II) and form complexes before they transfer to the bulk solution to form soluble ($FeCl_2$) and continues the dissolution.

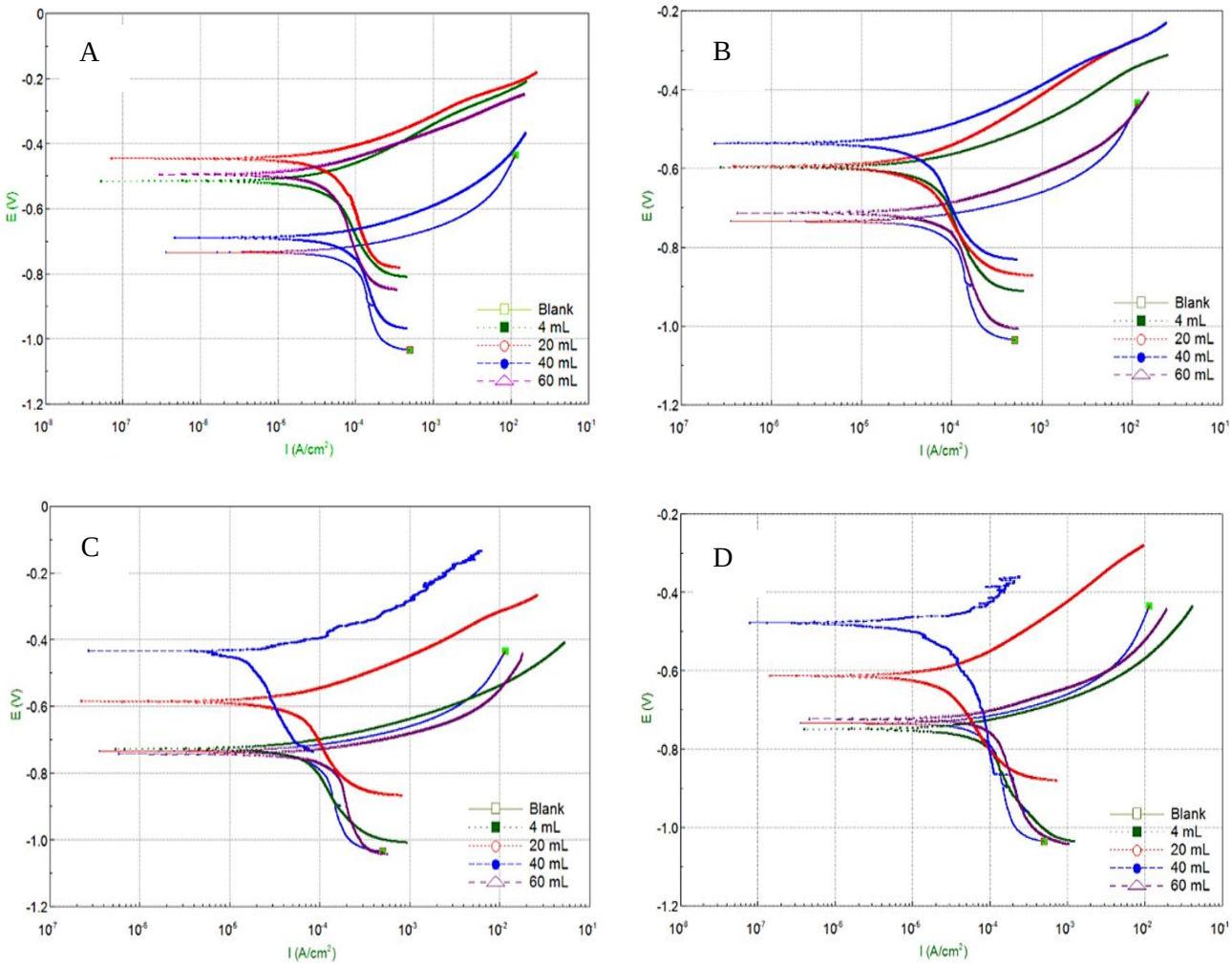

Figure 2: Polarization behavior for inhibition by (Dexon) drug at four different temperatures; (A) 303 K, (B) 313 K, (C) 323 K and (D) 333 K.

The data of corrosion/inhibition are listed in Table 1 indicating that the presence of Dexon drug in the solution generally shifts the corrosion potential to a nobler direction (i.e., Dexon is an anodic inhibitor) with lowering the corrosion current density as well as decreasing almost Tafel slopes compared with the blank case. The results of polarization resistance (R_p) using the measured data of polarization curves shows increasing resistance, especially in the presence of ($60\ mL/L$) of Dexon drug, also this concentration gave the highest inhibition efficiency ($IE\%$) that reached the range of 92.57 – 95.57% for decreasing temperature from 333 K to 303 K respectively.

Table 1: Corrosion/Inhibition data by (Dexon) at different concentrations and temperatures.

Conc. Of Actifed	Temp. (K)	-Ecorr (V)	icorr ($A.cm^{-2}$)	-bc ($mV.dec^{-1}$)	+ba ($mV.dec^{-1}$)	Rp×10^{-3} ($\Omega.cm^2$)	IE (%)
Blank	303	0.735	12.17	848.56	71.055	2.34	---
	313	0.744	13.36	831.8	70.235	2.10	---
	323	0.581	15.67	3933.1	96.846	2.62	---
	333	0.746	16.56	745.05	65.564	1.58	---
4 mL/L	303	0.528	2.69	719.34	124.00	17.07	77.88
	313	0.584	3.77	556.03	113.46	10.85	71.72
	323	0.620	5.07	100.78	98.366	4.26	67.61
	333	0.650	5.53	77.233	85.174	3.18	66.55

20 mL/L	303	0.473	0.79	37.008	28.322	8.82	93.44
	313	0.578	1.17	49.331	35.129	7.61	91.22
	323	0.610	1.36	32.735	30.869	5.07	91.27
	333	0.643	1.41	28.892	27.862	4.37	91.46
40 mL/L	303	0.522	0.98	41.242	34.402	8.31	91.91
	313	0.580	1.28	32.45	36.288	5.81	90.37
	323	0.617	2.26	69.27	33.123	4.31	85.55
	333	0.632	2.77	32.459	28.079	2.36	83.24
60 mL/L	303	0.482	0.53	46.69	97.419	25.86	95.57
	313	0.601	0.66	38.755	51.827	14.59	95.01
	323	0.622	0.94	19.402	44.087	6.22	93.98
	333	0.645	1.23	51.665	24.227	5.82	92.57

3.2.Supported Measurements

These measurements were done to confirm the inhibitive role of the added Dexon drug represented by FTIR, SEM, and AFM techniques. The infrared spectrum identifies the nature of different bonds in the drug's molecule that has a broad band at 3296 cm^{-1} corresponding to stretching of $(O-H)$ bond followed by the medium band at 1639 cm^{-1} related to stretching of $(C=O)$ bond and then at 1414 cm^{-1} corresponded to stretching of $(C=C)$ bond, also can be seen in the stretching of $(C-F)$ bond as small band at 1042 cm^{-1}, as in Fig. 3a. After the Corrosion/Inhibition process, the film formed on carbon steel substrate was subjected to FTIR analysis at a concentration of 60 mL/L to obtain the spectrum as in Fig. 3b which illustrates the decrease in almost all peaks, especially $(O-H)$ group. This indicates that all the functional groups in the Dexon molecule participated in the adsorption process, resulting in effective surface coverage and form ($Fe^{2+}-$ Dexamethasone complex) through orienting the $(O-H)$ and $(C=O)$ toward (Fe^{2+}) at the electrical double layer as a suggested mechanism in (see Fig. 4).

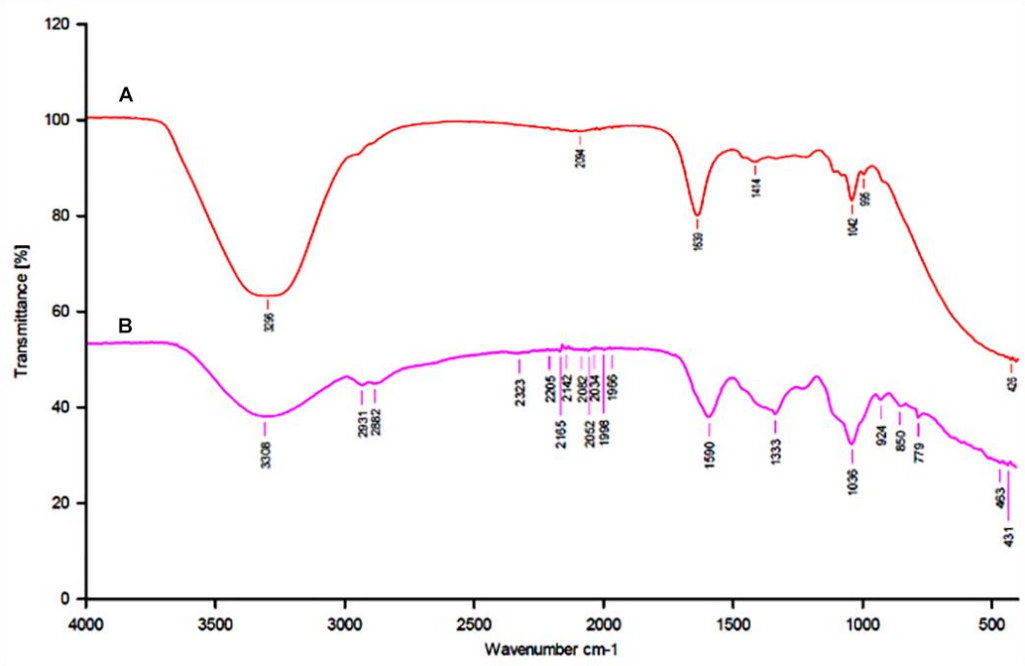

Figure 3: FTIR spectra for (A) Dexon drug, and (B) a film formed after inhibition.

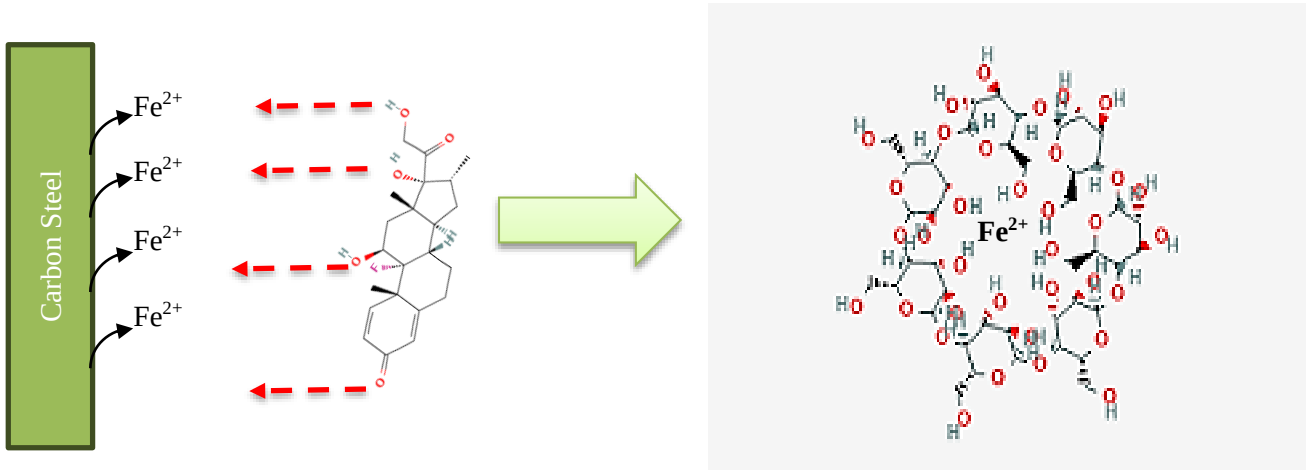

Figure 4: Schematic mechanism of Iron (II)-Dexon coordinated complex.

Scanning electron microscopy (SEM) was also used to identify the corroded and inhibited surface in Fig. 5 and Fig. 6 at two magnifications respectively. Images in Fig. 5 indicate the corrosion sites (Anodic & Cathodic) with corrosion products such as iron oxides (Fe_2O_3 & Fe_3O_4) with iron chlorides ($FeCl_2, FeOHCl, FeCl_3, FeOHCl_2, FeOH_2Cl$ and $FeCl_3^-$), while in Fig. 6 the images show the coverage by adsorbed layer from attraction drug molecules to the metallic surface. The bulky molecules of the Dexon drug appear as clusters with large cohesive particles as illustrated by Nikhil *et al*. [47] when they studied the release of (Dexamethasone) from microcapsules using SEM examination.(see Fig. 5) also shows the fusion of drug particles forming syncytium-like aggregates, resulting in compact, dense coverage that effectively covers the surface, providing strong protection.

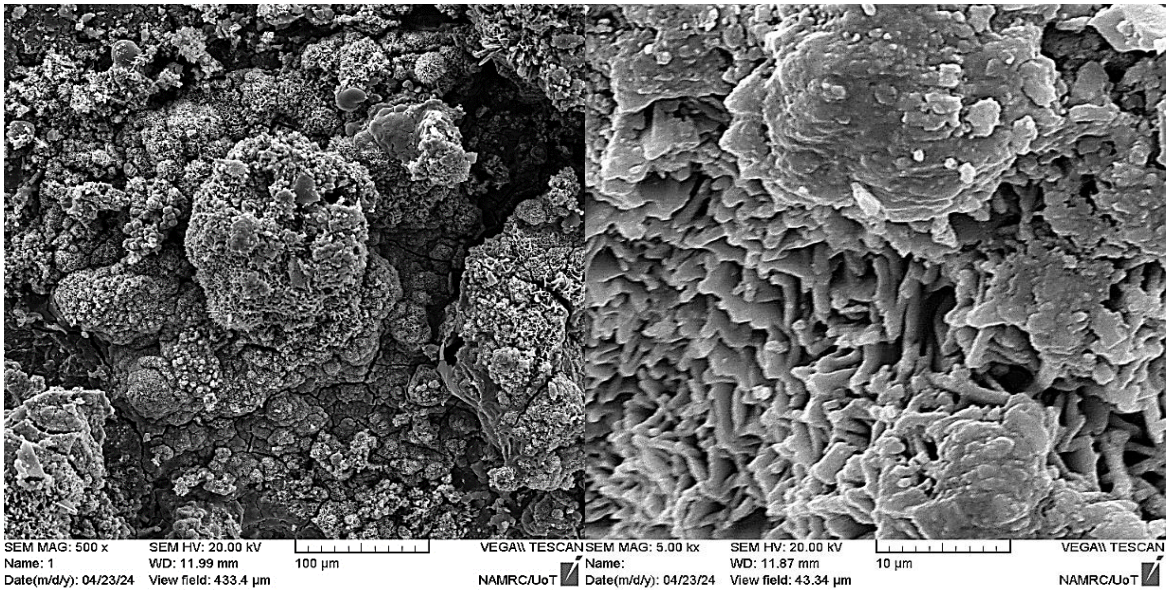

Figure 5. SEM images for corroded samples in seawater solution.

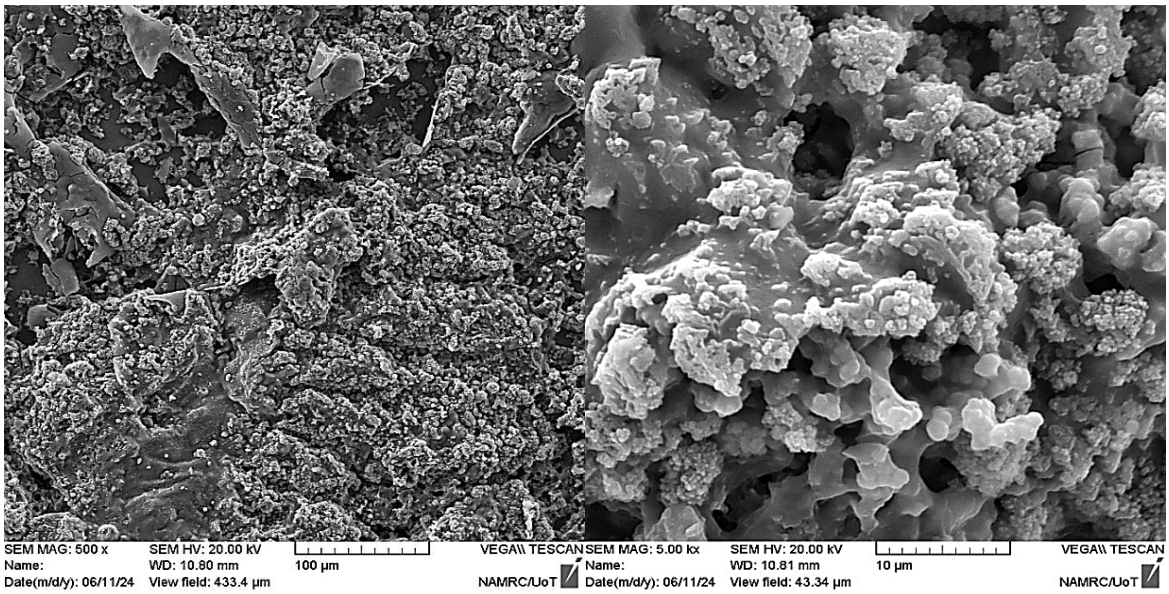

Figure 6. SEM images for inhibited samples in seawater solution with 60 mL/L Dexon.

The examination by atomic force microscopy is also important to confirm the coverage by inhibited Dexon drugs. In Fig. 7, can be seen the big mountains covered the corroded surface due to different corrosion products in sodium chloride medium confirming the formation of cathodic and anodic sites to give surface roughness equal to 270.8 nm with coverage of (64.22 %) and mean diameter reach to 56.42 nm due to small particles of formed oxides and salts. In Fig. 8, a smoother surface can be seen due to coverage by (Fe^{2+} − Dexamethasone) complex that gives bulky, dense, impact and homogeneous particles with surface roughness equal to 24.96 nm and coverage of (23.32 %), because of the bulky complex, the mean diameter reached 75.92 nm.

The surface volume parameters shown in Fig. 9 demonstrate reduced void volume and pit volume after inhibition. The void volume decreased from 378.8 nm in corroded specimens to 92.29 nm in inhibited specimens, while the pit volume reduced from 44.70 nm to 10.85 nm, respectively.

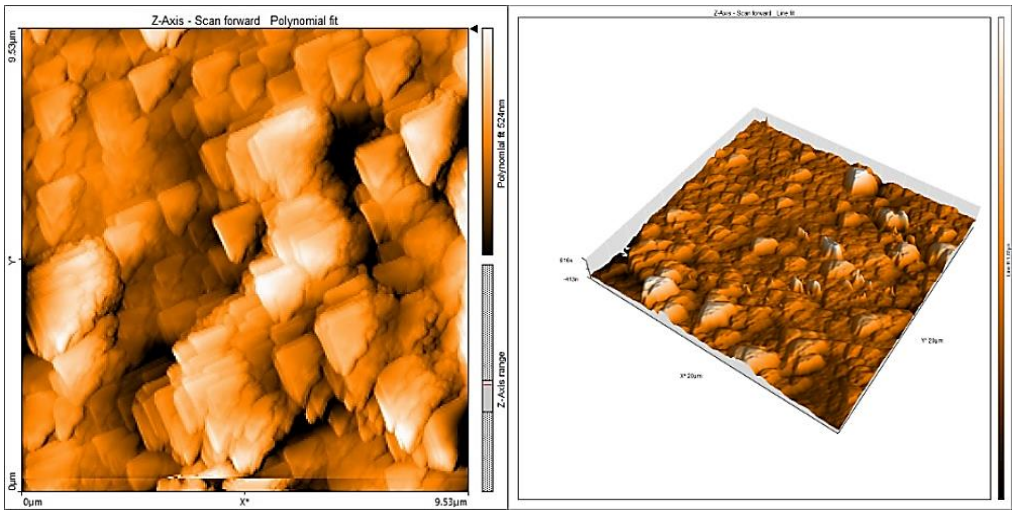

Figure 7: 2D and 3D images for the corroded surface.

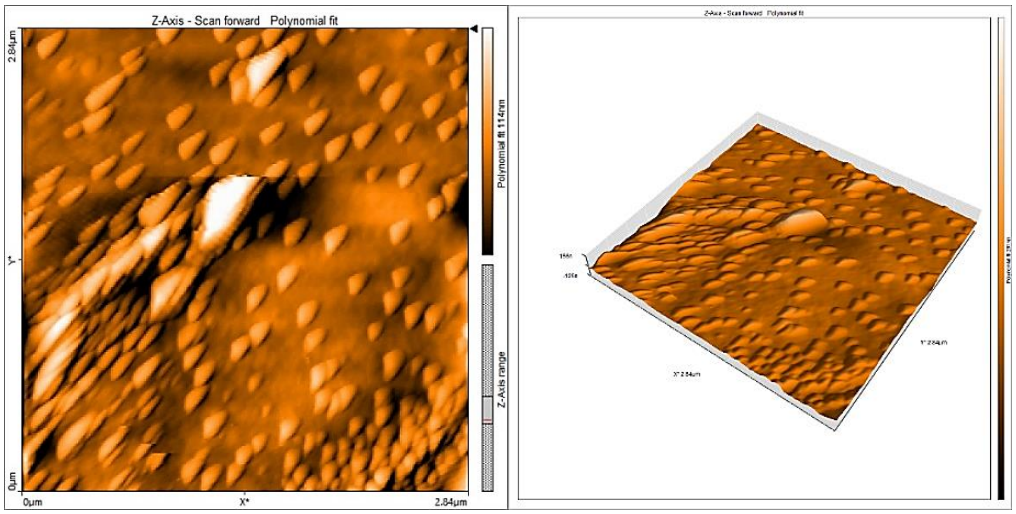

Figure 8: $2D$ and $3D$ images for the inhibited surface.

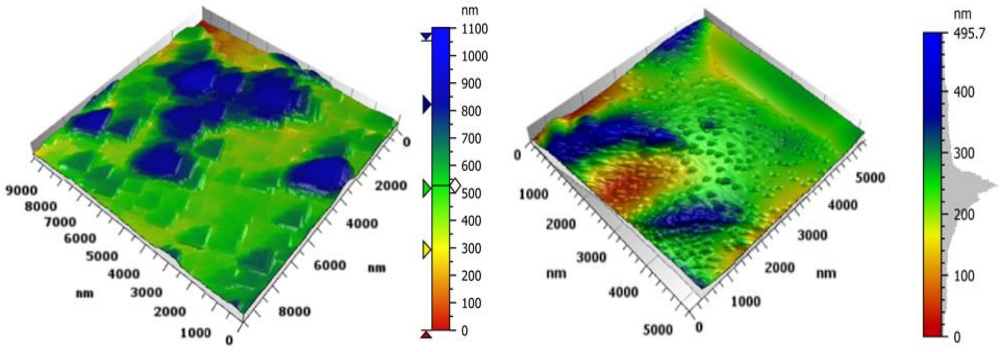

Figure 9: $3D$ views for volume analysis corroded (a) and inhibited (b) surface.

3.3.Supported Calculations

3.3.1.Adsorption Properties

The calculations related to the adsorption of Dexon confirm the inhibition process according to the nature, type, size, and charge of inhibitor molecules. The data in Table 2 illustrate the small values for the adsorption-desorption constant indicating the physical kind of adsorption on carbon steel surface by Dexon molecules associated with negative values of Gipps free energy for this adsorption especially by higher concentrations (40 & 60 mL/L). The straight lines in Fig. 10 for the relation between (C_{Drug}) and (C_{Drug}/θ) with (R^2) close to unity, where recorded (0.9928), (0.9949), (0.9989) and (0.9993) at (303), (313), (323), and (333) Kelvin respectively, suggesting that Dexon drug as inhibitor follows the Langmuir isotherm theory. This theory assumes that each water molecule at the electrical double layer is replaced by an inhibitor molecule, forming a barrier that reduces corrosion on the metallic surface.

As listed in Table 2, the thermodynamic data for adsorption show negative free energy values, indicating a spontaneous process. Negative entropy values were also recorded, which are attributed to the formation of a stable complex (Fe^{2+} – Dexamethasone) This complex has an associative nature, minimizing the movement of (Fe^{2+} & Cl^{-}) ions on the surface. Additionally, the negative enthalpy values in Table 2 and Fig. 11, which are less than -20 kJ/mol, confirm that the adsorption process is exothermic and involves physical adsorption of the Dexon drug.

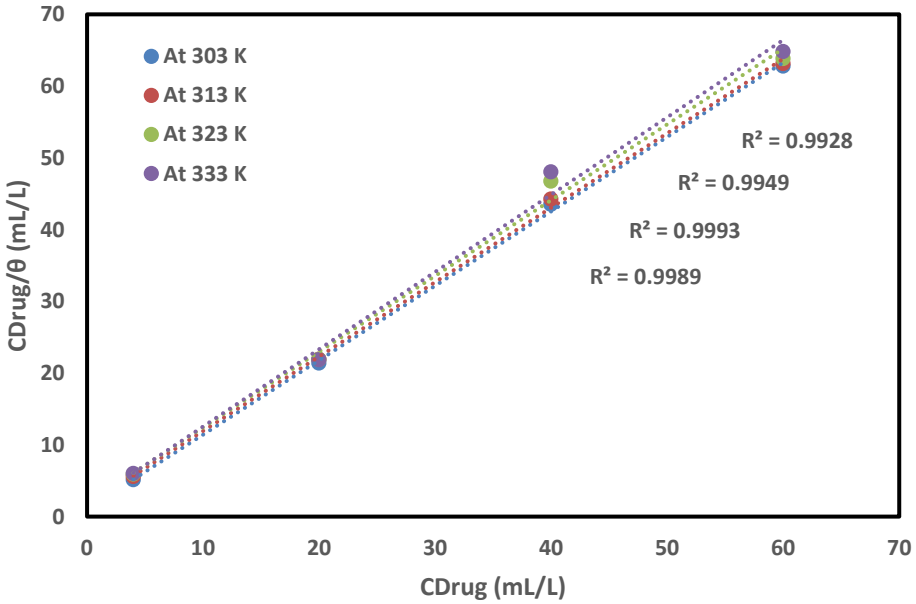

Figure 10. Langmuir isotherm theory for Dexon adsorption.

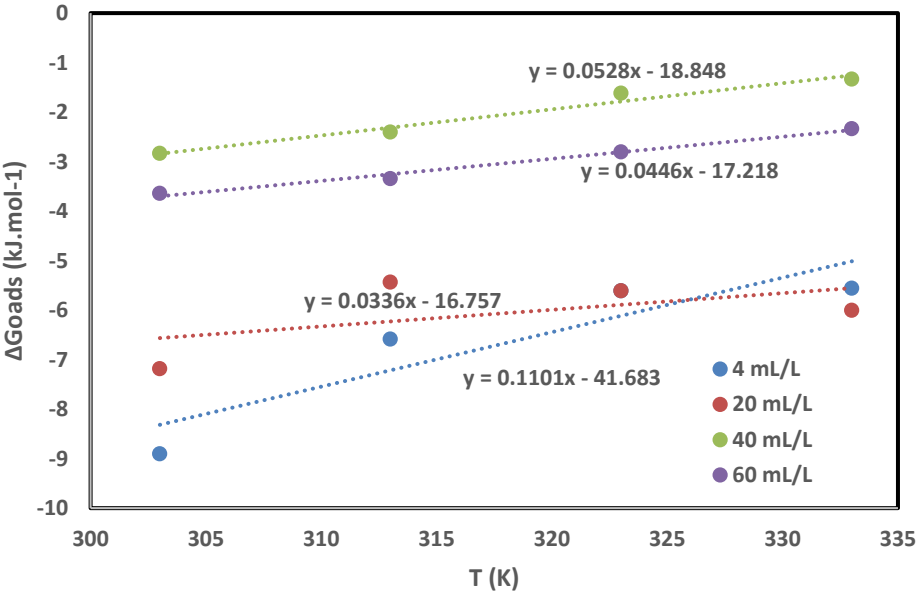

Figure 11: The relation between free energy (ΔG^{o}_{ads}) and temperature (T).

Table 2: Isotherm data of inhibition by Dexon drug.

Conc. (mL/L)	Temp. (K)	K_{ads} L/mL	$-\Delta G^{o}_{ads}$ kJ.mol^{-1}	$-\Delta S^{o}_{ads}$ J.mol^{-1}	$-\Delta H^{o}_{ads}$ kJ.mol^{-1}
4	303	0.88	8.905	0.11012	9.092
	313	0.63	6.586		6.780
	323	0.52	5.609		5.809
	333	0.50	5.560		5.766
20	303	0.71	7.185	0.03364	2.885
	313	0.52	5.436		2.457

	323	0.52	5.609		1.672
	333	0.54	6.006		1.391
40	303	0.28	2.834	0.05283	2.858
	313	0.23	2.404		2.429
	323	0.15	1.618		1.643
	333	0.12	1.335		1.361
60	303	0.36	3.643	0.04461	0.033
	313	0.32	3.345		0.031
	323	0.26	2.805		0.027
	333	0.21	2.336		0.023

3.3.2 Energic and Electronic Properties

This study was done on a component of a Dexon drug called Dexamethasone to investigate its electronic properties as a corrosion inhibitor using Time-Dependent Density Functional Theory (TD-DFT). The optimized geometry is shown in Fig. 12, The energetic properties of Dexon, listed in Table 3, include total energy, LUMO energy (which indicates the ability to accept electrons from the metal through antibonding orbitals and saturated bonds), HOMO energy (which reflects the tendency to donate electrons to an empty orbital), and the energy gap ΔE. A lower ΔE suggests better inhibitor activity and a softer molecule [48], the high value of ($E_{LUMO} = -1.6892$) confirm the activity of Dexon as an inhibitor.

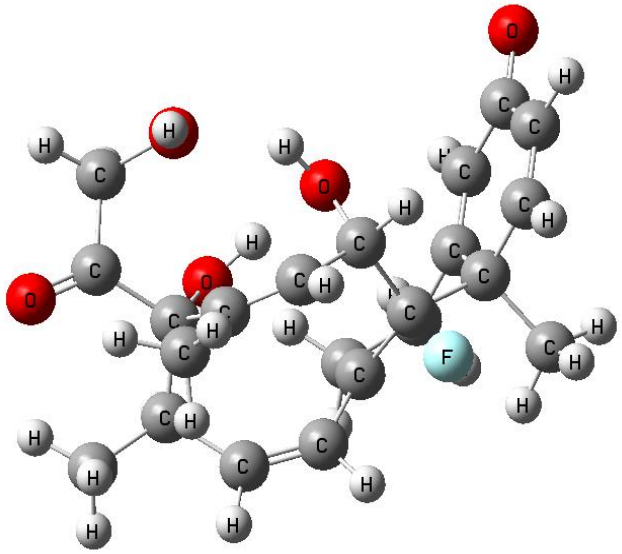

Figure 12: $B3LYP/6-31G$ optimized geometries of (Dexamethasone).

Table 3: The energic properties for (Dexamethasone) by the DFT at the B3LYP/6-311G level.

Total Energy (a.u.)	E_{HOMO} (eV)	E_{LUMO} (eV)	Energy gap (eV)
-1329.4324	-5.1715	-1.6892	3.482

The electronic properties are listed in Table 4, where (η and σ) are related to the stability and reactivity of the Dexamethasone molecule [44] and they confirm the high basicity and high ability for electron donating in addition to the soft nature as mentioned above through the value of (ΔE) [49]. The large value of the energy gap (ΔE) reflects the complex nature of the molecule and the low value refers to the soft one [44], the value of (3.4303 eV) for electronegativity (χ) confirms the inhibitive role of Dexon drug followed by the negative value of chemical

potential (μ) that suggests the releasing energy for the reaction. Also, The ability of a molecule (drug) to attract electrons within a chemical bond can be expressed through its electrophilicity index (ω). When a fluorine (F) atom is present along with oxygen (O) atoms in various functional groups, this can be observed by examining the fraction of electrons (ΔN) value, as shown in Table 4. This value represents the amount of electron transfer to the acceptor [50] which correlates with the molecule's capacity to interact with a metallic surface, such as carbon steel. This interaction is also linked to the molecule's dipole moment (D) value [51]. Fig. 13 illustrates the active sites in the Dexon drug structure characterized by their energy differences (ΔE), which indicate their potential for playing a significant role in the drug's inhibitory effectiveness. These sites are likely candidates for contributing to the drug's inhibitive function.

Table 4: The electronic properties for (Dexamethasone) in eV unit.

η	σ	χ	$-\mu$	ω	ΔN	D
1.7411	0.2871	3.4303	3.4303	3.3791	1.0251	4.7185

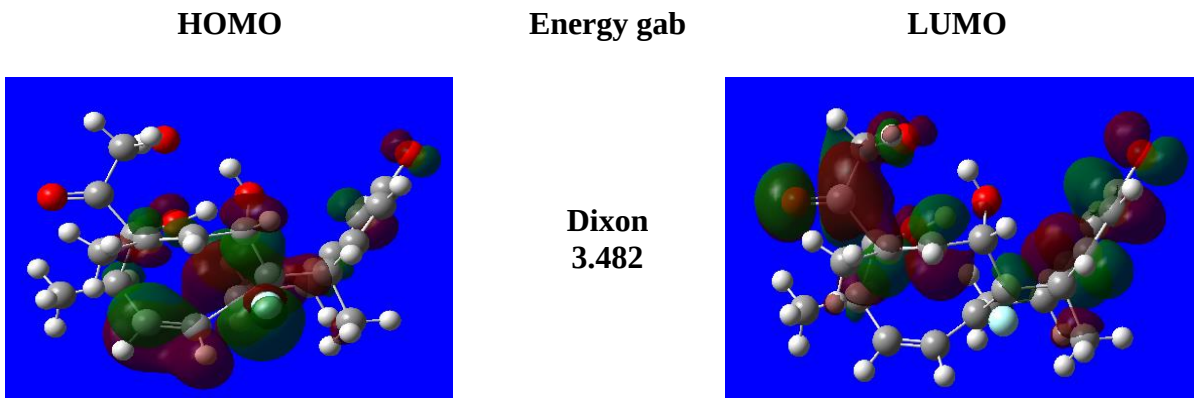

Figure 13: B3LYP/6-31G HOMO and LUMO of Dexon.

Finally, the feature of the molecular electrostatic potential (MEP) is shown in Fig. 14 labeled with different colours beginning from the red color regions as electron−rich sites (i.e., O) to reach the blue color regions as electron−poor sites that have disappeared in the Dexamethasone structure confirming the inhibitive role for Dexon drug. Also, the net electrostatic effects are shown in the surrounding spaces of the molecule with a total charge distribution as nuclei and electrons [52-54], In the Fig. 14, five oxygen atoms took the most active electrophilic sites with the MEP ranged from $-7.395e-2$ a. u. (red) to $+7.395e-2$ a. u. (blue) on the surface mapping.

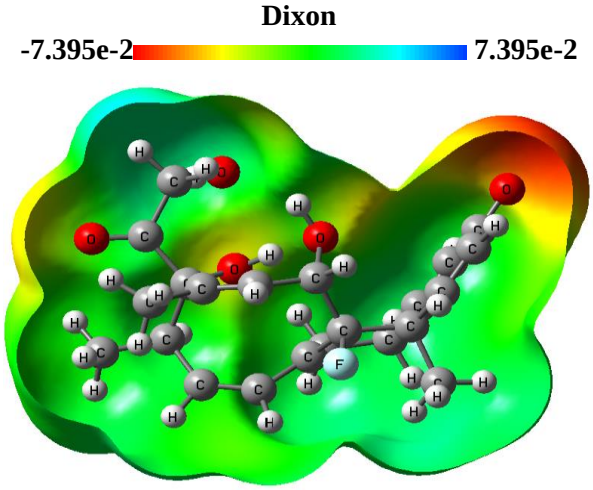

Figure 14: Molecular electrostatic potentials (MEP) of Dexon drug.

4. Conclusions

The Dexon drug, composed of the Dexamethasone molecule, acts as an effective green inhibitor for carbon steel in simulated seawater solutions across varying concentrations (4 to 60 mL/L) and temperatures (303 to 333 K). Electrochemical tests showed promising results in terms of polarization resistance and inhibition efficiency. SEM and AFM analyses revealed that the drug formed a protective layer on the steel surface due to complexes between iron ions and drug molecules, a finding further supported by FTIR spectroscopic data. The adsorption analysis indicated physical adsorption with negative values for free energy, entropy, and enthalpy, following the Langmuir isotherm. Additionally, energetic and electronic properties confirmed the presence of active sites in the drug molecule, supporting its effectiveness as an inhibitor based on quantum calculations.

Conflict of Interest

The authors declare that they have no conflict of interest.

References

[1] M. H. Hafiz, R. A. Majed, R. S. Noor, and M. A. Wehib, "Phenylenediamine as inhibitor in sour water at oil refinery," *Int. J. Electrochem. Sci.*, vol. 8, no. 12, pp. 12402–12416, 2013.

[2] Z. S. Aziz, R. A. Majed, M. H. Abd, and S. A. Naser, "Corrosion inhibition of carbon steel in seawater solution by wild clary extracts," in *AIP Conference Proceedings*, AIP Publishing, 2023.

[3] N. O. Eddy, S. R. Stoyanov, and E. E. Ebenso, "Fluoroquinolones as corrosion inhibitors for mild steel in acidic medium; experimental and theoretical studies," *Int. J. Electrochem. Sci.*, vol. 5, no. 8, pp. 1127–1150, 2010.

[4] N. O. Eddy and E. E. Ebenso, "Corrosion inhibition and adsorption characteristics of tarivid on mild steel in H2SO4," *J. Chem.*, vol. 7, pp. S442–S448, 2010.

[5] R. S. A. Hameed, "Ranitidine drugs as non-toxic corrosion inhibitors for mild steel in hydrochloric acid medium," *Port Electrochim Acta*, vol. 29, no. 4, pp. 273–285, 2011.

[6] I. Naqvi, A. R. Saleemi, and S. Naveed, "Cefixime: A drug as Efficient Corrosion Inhibitor for Mild Steel in Acidic Media. Electrochemical and Thermodynamic Studies.," *Int. J. Electrochem. Sci.*, vol. 6, no. 1, pp. 146–161, 2011.

[7] M. Abdallah, I. Zaafarany, S. O. Al-Karanee, and A. A. Abd El-Fattah, "Antihypertensive drugs as an inhibitors for corrosion of aluminum and aluminum silicon alloys in aqueous solutions," *Arab. J. Chem.*, vol. 5, no. 2, pp. 225–234, 2012.

[8] A. S. Fouda, M. N. El-Haddad, and Y. M. Abdallah, "Septazole: antibacterial drug as a green corrosion inhibitor for copper in hydrochloric acid solutions," *Int. J. Innov. Res. Sci. Eng. Technol.*, vol. 2, no. 12, pp. 7073–7085, 2013.

[9] A. S. Fouda, M. A. Elmorsi, T. A. Fayed, A. F. Hassan, and M. Soltan, "Corrosion inhibitors based on antibiotic derivatives for protection of carbon steel corrosion in hydrochloric acid solutions," *Int. J. Adv. Res.*, vol. 2, no. 4, pp. 788–807, 2014.

[10] A. S. Fouda and H. E. Gadow, "Streptoquin and Septazole: Antibiotic drugs as corrosion inhibitors for copper in aqueous solutions," *Glob. J. Res. Eng.*, vol. 14, no. 2, pp. 22–36, 2014.

[11] A. S. Mahdi, "Amoxicillin as green corrosion inhibitor for concrete reinforced steel in simulated concrete pore solution containing chloride," *Int. J. Adv. Res. Eng. Technol.*, vol. 5, pp. 99–107, 2014.

[12] I. A. Akpan and N. O. Offiong, "A modiaquine drug as a corrosion inhibitor for mild steel in 0.1 M HCl solution," *Chem. Met. Alloy.*, no. 7,№ 3–4, pp. 149–153, 2014.

[13] R. S. A. Hameed, E. A. Ismail, A. H. Abu-Nawwas, and H. I. Al-Shafey, "Expired Voltaren drugs as corrosion inhibitor for aluminium in hydrochloric acid," *Int. J. Electrochem. Sci.*, vol. 10, no. 3, pp. 2098–2109, 2015.

[14] P. O. Ameh and U. M. Sani, "Cefuroxime axetil: A commercially available pro-drug as corrosion inhibitor for aluminum in hydrochloric acid solution," *J. Heterocycl.*, vol. 101, pp. 1–6, 2015.

[15] E. M. Attia, "Expired Farcolin drugs as corrosion inhibitor for carbon steel in 1 M HCl solution," *J. Basic Appl. Chem.*, vol. 5, no. 1, pp. 1–15, 2015.

[16] M. Abdallah, I. A. Zaafarany, and B. A. Al Jahdaly, "Corrosion inhibition of zinc in hydrochloric acid using some antibiotic drugs," *J. Mater. Environ. Sci*, vol. 7, no. 4, pp. 1107–1118, 2016.

[17] N. H. Ramadan and F. El Aal Abd Nadia, "Unused augmentin drug as save corrosion inhibitor for α-brass

in nitric acid solution," *Zast. Mater.*, vol. 57, no. 2, pp. 326–338, 2016.
[18] R. J. Aziz, "Study of some drugs as corrosion inhibitors for mild steel in 1M H2SO4 solution," *Int. J. Curr. Res. Chem. Pharm. Sci*, vol. 3, no. 12, pp. 1–7, 2016.
[19] M. M. Motawea, H. S. Gadow, and A. S. Fouda, "Expired Cidamex drug as corrosion inhibitor for aluminum in acidic solution," *Glo. J. Res. Eng. Chem. Eng*, vol. 16, pp. 7–19, 2016.
[20] A. S. Fouda, S. M. Rashwan, M. Kamel, and A. A. Badawy, "Unused meropenem drug as corrosion inhibitor for copper in acidic medium; experimental and theoretical studies," *Int. J. Electrochem. Sci.*, vol. 11, no. 11, pp. 9745–9761, 2016.
[21] P. Singh, D. S. Chauhan, K. Srivastava, V. Srivastava, and M. A. Quraishi, "Expired atorvastatin drug as corrosion inhibitor for mild steel in hydrochloric acid solution," *Int. J. Ind. Chem.*, vol. 8, pp. 363–372, 2017.
[22] D. K. Verma and F. Khan, "Corrosion inhibition of mild steel by using sulpha drugs in phosphoric acid medium: a combined experimental and theoretical approach," *Am Chem Sci J*, vol. 14, no. 3, pp. 1–8, 2016.
[23] C. Verma, D. S. Chauhan, and M. A. Quraishi, "Drugs as environmentally benign corrosion inhibitors for ferrous and nonferrous materials in acid environment: an overview," *J. Mater. Environ. Sci*, vol. 8, no. 11, pp. 4040–4051, 2017.
[24] M. E. Ikpi, F. E. Abeng, and B. O. Okonkwo, "Experimental and computational study of levofloxacin as corrosion inhibitor for carbon steel in acidic media," *World News Nat. Sci.*, no. 9, pp. 79–90, 2017.
[25] R. A. Anaee, I. H. R. Tomi, M. H. Abdulmajeed, S. A. Naser, and M. M. Kathem, "Expired Etoricoxib as a corrosion inhibitor for steel in acidic solution," *J. Mol. Liq.*, vol. 279, pp. 594–602, 2019.
[26] R. A. Anaee, M. H. Abd Al-Majeed, S. A. Naser, M. M. Kathem, and O. A. Ahmed, "Antibacterial inhibitor as an expired metoclopramide in 0.5 M phosphoric acid," *Al-Khwarizmi Eng. J.*, vol. 15, no. 1, pp. 71–81, 2019.
[27] A. M. Kadhim, R. A. Anaee, M. J. M. Hassan, and M. A. I. Al-lami, "Study the corrosion inhibition on the Iraqi fuel tanks using Cefoperazone Drug," *Al-Mustansiriyah J. Sci.*, vol. 34, no. 3, pp. 31–42, 2023.
[28] T. A. Alkarim, K. F. Al Azawi, and R. A. Anaee, "GREEN APPROACH TO CORROSION INHIBITION OF ALUMINUM IN ACIDIC SOLUTIONS BY THE EXPIRE DRUG AND BIOLOGICAL ACTIVITY.," *Biochem. Cell. Arch.*, vol. 21, no. 2, 2021.
[29] T. A. Alkarim, K. F. Al-Azawi, and R. A. Anaee, "Anticorrosive properties of Spiramycin for aluminum in acidic medium," *Int. J. Corros. Scale Inhib.*, vol. 10, no. 3, pp. 1168–1188, 2021.
[30] T. Abd Alkarim, K. F. Al-Azawi, and R. A. Anaee, "Experimental study and quantum calculations for spiramycin and isosorbide dinitrate as corrosion inhibitors," *J. Appl. Sci. Nanotechnol.*, vol. 3, no. 1, pp. 18–33, 2023.
[31] H. A. Abdullah, R. A. Anaee, and A. A. Khadom, "Expired Metheprim drug as a corrosion inhibitor for aluminum in 1 M HCl solution: Experimental and theoretical studies," *Int. J. Corros. Scale Inhib*, vol. 11, pp. 1355–1373, 2022.
[32] M. S. Abdul, R. Anaee, and T. Mathew, "Negative effect of calcium tablets on the corrosion of a Co–Cr–Mo alloy as an implant," *Int J Corros Scale Inhib*, vol. 12, pp. 275–291, 2023.
[33] S. A. A. Maged, R. A. Anaee, and M. T. Mathew, "The Role of Uric Acid to Reduce the Corrosion of Co-Cr-Mo Alloy as Joint in Presence of Ca and Vitamin D3," *J. Bio-and Tribo-Corrosion*, vol. 9, no. 4, p. 66, 2023.
[34] A. M. H. Al-Ghaban, H. A. Abdullah, R. A. Anaee, S. A. Naser, and A. A. Khadom, "Expired butamirate drug as eco-friendly corrosion inhibitor for aluminum in seawater: Experimental and theoretical studies," *J. Eng. Res.*, vol. 12, no. 3, pp. 299–309, 2024.
[35] R. A. M. Anaee, "Thermodynamic and kinetic study for corrosion of Al-Si-Cu/Y2O3 composites," *Asian J. Chem.*, vol. 26, no. 14, pp. 4469–4474, 2014.
[36] N. Najm, A. H. Ataiwi, and R. A. Anaee, "Annealing and coating influence on the mechanical properties, microstructure, and corrosion properties of biodegradable Mg alloy (AZ91)," *J. Bio-and Tribo-Corrosion*, vol. 8, no. 2, p. 64, 2022.
[37] S. A. Naser, R. A. Anaee, and H. A. Jaber, "Gd–Ni–Ti coating to reduce corrosion of SS 316L for bioapplication," *Adv. Mater. Process. Technol.*, pp. 1–12, 2024.
[38] S. Naser, R. Anaee, and H. Jaber, "In Vitro and In Vivo Study for Behavior of Coated SS 316 L with

SmNiTi and GdNiTi by DC Sputtering," *Chem. Africa*, vol. 7, no. 3, pp. 1303–1310, 2024.
[39] N. Najm, A. H. Ataiwi, and R. A. Anaee, "Effect of indium coating on corrosion behavior of AZ31 Mg alloy by DC sputtering," *Mater. Today Proc.*, vol. 62, pp. 4551–4555, 2022.
[40] R. A. Anaee, "Behavior of Ti/HA in saliva at different temperatures as restorative materials," *J. Bio-and Tribo-Corrosion*, vol. 2, pp. 1–9, 2016.
[41] H. A. Abdullah, R. A. Anaee, A. A. Khadom, A. T. Abd Ali, A. H. Malik, and M. M. Kadhim, "Experimental and theoretical assessments of the chamomile flower extract as a green corrosion inhibitor for aluminum in artificial seawater," *Results Chem.*, vol. 6, p. 101035, 2023.
[42] S. S. Hamdi, H. H. Al-Kayiem, A. S. Muhsan, and E. Magaril, "Experimental dataset on the dispersion stability of natural polymer non-covalently functionalized graphene nanoplatelets in high salinity brines," *Èlektronnyj Arh.*, vol. 31, p. 105702, Aug. 2020, doi: 10.1016/j.dib.2020.105702.
[43] A. A. Issa and H. R. Obayes, "Capture carcinogenic aromatic compounds by the design of new tweezer compounds: a theoretical study," *J. Mol. Model.*, vol. 26, no. 10, p. 292, 2020.
[44] A. A. Issa, M. D. Kamel, and D. S. El-Sayed, "Depicted simulation model for removal of second-generation antipsychotic drugs adsorbed on Zn-MOF: adsorption locator assessment," *J. Mol. Model.*, vol. 30, no. 4, p. 106, 2024.
[45] W. J. Pietro, M. M. Francl, W. J. Hehre, D. J. DeFrees, J. A. Pople, and J. S. Binkley, "Self-consistent molecular orbital methods. 24. Supplemented small split-valence basis sets for second-row elements," *J. Am. Chem. Soc.*, vol. 104, no. 19, pp. 5039–5048, 1982.
[46] K. D. Dobbs and W. J. Hehre, "Molecular orbital theory of the properties of inorganic and organometallic compounds 5. Extended basis sets for first-row transition metals," *J. Comput. Chem.*, vol. 8, no. 6, pp. 861–879, 1987.
[47] N. Pargaonkar, Y. M. Lvov, N. Li, J. H. Steenekamp, and M. M. de Villiers, "Controlled release of dexamethasone from microcapsules produced by polyelectrolyte layer-by-layer nanoassembly," *Pharm. Res.*, vol. 22, pp. 826–835, 2005.
[48] H. Ibraheem, Y. Al-Majedy, A. A. Issa, and E. Yousif, "Photostabilization, Thermodynamic and Theoretical Studies of polystyrene by some 2-amino pyridine," *Trends Sci.*, vol. 21, no. 2, p. 7374, 2024.
[49] A. A. Issa, H. H. Ibraheem, and D. S. El-Sayed, "Computational innovation of in situ metallic elements with zirconia as a novel possible carrier for chemotherapeutic medication," *J. Mol. Model.*, vol. 30, no. 1, p. 14, 2024.
[50] Y. K. Al-Majedy, H. H. Ibraheem, and A. A. Issa, "Antioxidant, antimicrobial activity and quantum chemical studies of 4-methyl-7-hyroxy coumarin derivatives," in *AIP Conference Proceedings*, AIP Publishing, 2023.
[51] H. H. Ibraheem, A. A. Issa, and D. S. El-Sayed, "Structural behavior and surface layer modification of (E)-N'-((1H-indol-3-yl) methylene)-4-chlorobenzohydrazide: Spectroscopic, DFT, biomedical activity and molecular dynamic simulation against Candida Albicans receptor," *J. Mol. Struct.*, vol. 1312, p. 138484, 2024.
[52] P. G. Magar, R. Uprety, and K. B. Rai, "First-Principles DFT Study of the Molecular Structure, Spectroscopic Analysis, Electronic Structures and Thermodynamic Properties of Ascorbic Acid," *Himal. Phys.*, vol. 11, 2024.
[53] M. I. Sayyed, K. M. Kaky, and R. A. Anaee, "Chromium ions effects on Sb2O3-PbO-GeO2 glass properties for radiation protection," *J. Theor. Appl. Phys.*, vol. 18, no. 1, 2024.
[54] U. Ishtiaq, A. Aref, A. S. Muhsan, A. Rashid, and S. S. Hamdi, "High strength glass beads coated with CNT/rGO incorporated urethane coating for improved crush resistance for effective hydraulic fracturing," *J. Pet. Explor. Prod. Technol.*, vol. 12, no. 10, pp. 2691–2697, 2022.